Research Article

Direction-of-Arrival Estimation for 2D Coherently Distributed Sources with Nested Array Based on Matrix Reconstruction

Yu Xiao,[1] Tao Wu [ORCID],[2] Yiwen Li,[3] Xinping Ma,[4] and Yijie Huang[1]

[1]*School of Automation, Northwestern Polytechnical University, Xi'an 710072, Shaanxi, China*
[2]*Equipment Management and UAV College, Air Force Engineering University, Xi'an 710051, Shaanxi, China*
[3]*Aeronautical Engineering College, Air Force Engineering University, Xi'an 710051, Shaanxi, China*
[4]*College of Resources, Environment and History and Culture, Xianyang Normal University, Xianyang 712000, Shaanxi, China*

Correspondence should be addressed to Tao Wu; taowu_nwpu@126.com

This paper has made proposition of a nested array and an estimation algorithm for direction-of-arrival (DOA) of two-dimensional (2D) coherently distributed (CD) sources. According to the difference coarray concept, double parallel hole-free virtual uniform linear arrays are generated by virtue of vectorization operation on cross-correlation matrices of subarrays. Sensor coordinates of virtual arrays are derived. Rational invariance relationships of virtual arrays are derived. According to the rotational invariance relationships, matrices satisfying rotation invariance are constructed by extracting and regrouping the receive vectors of the virtual arrays, and then an estimation of signal parameters via rotational invariance techniques- (ESPRIT-) like framework on matrix reconstruction is deduced. Optimal configuration of the nested array as well as computational complexity are analyzed. Without pair matching, the proposed method can resolve more sources than the sensor number. Simulation outcomes indicate that the proposed method tends to have a better performance as compared to the traditional uniform arrays that have similar number of sensors.

1. Introduction

Traditional direction-of-arrival (DOA) estimators consider a target as a point source. In underwater acoustic detection, with the reduction of the distance between the receive array and a target, as many parts of the target reflect signals; a point source model cannot describe the target effectively and the supposed conditions of a point source model are invalid. In this case, a distributed source model is proposed [1]. A distributed source can be considered as an aggregation of point sources within a spatial distribution, where the point sources can be called scatterers.

Generally, distributed sources can be possibly categorized as incoherent distributed (ID) and coherent distributed (CD) sources according to the coherence of scatterers. The scatterers of an ID source can be assumed to be incoherent, while scatterers of a CD source are coherent. Distributed sources can be categorized into one-dimensional (1D) and two-dimensional (2D) according to the spatial distribution dimension. The 2D distributed sources with the assumption that scatterers of a distributed source and the receive array are not in a same plane is more general and accordant with practical circumstances. In this paper, we are concerned with 2D CD sources.

The distributions of scatterers of CD sources can be described by deterministic angular signal distribution function (ASDF). ASDF of a source can be modeled as Gaussian, uniform, or any other form of distribution based on the geometric and surface characteristics of the source. ASDF of a 1D CD source involves parameters which are nominal angle and angular spread. ASDF of a 2D source is described by nominal azimuth, nominal elevation, azimuth spread, and elevation spread. Nominal azimuth as well as nominal elevation are collectively called nominal angles representing the target centers; these can also be possibly presented as DOA. Azimuth spread and elevation spread are

called angular spreads denoting the spatial extension of a target.

Considering point sources, some important achievements of DOA estimation have been presented in a mixed signal field and multiangle estimation recently. The 2D DOA estimation problem for a mixture of circular and noncircular signals is considered based on two parallel uniform linear arrays (ULAs) [2] and the uniform rectangular array (URA) [3]. In [4], authors have achieved estimating 2D DOA, 2D direction-of-departure, 2D receive polarization angle, and 2D transmit polarization angle simultaneously under an electromagnetic vector sensor (EMVS) MIMO system. A dimensional reduction noncircular MUSIC algorithm with a low computational complexity is proposed in [5] for DOA and polarization estimation of circular and noncircular mixture signals in a virtual MIMO system. As for ID sources, 2D DOA estimation of ID sources in massive multiple-input multiple-output (MIMO) systems using URAs is proposed in [6].

As for CD sources, based on spectral search, several estimators have been provided from the classical point source technique multiple signal classification (MUSIC) such as distributed signal parameter estimator (DSPE) [1], dispersed signal parametric estimation (DISPARE) [7], and vec-multiple signal classification (vec-MUSIC) [8]. Shahbazpanahi et al. [9] have extended another classical point sources technique estimation of signal parameters via rotational invariance techniques (ESPRIT) to make an estimation of the nominal angles of sources in the first place and thereafter make calculations of the angular spreads by means of spectral search. Zoubir et al. have explored a generalized beamforming estimator in [10]. Xiong et al. [11] have analyzed the performance of DSPE algorithm considering that estimators for CD sources mostly approximate conclusions made on assumptions of small angular spreads. All these estimators are concerned on 1D CD sources where scatterers and receive arrays are in the same plane. However, scatterers and arrays are in three-dimensional space generally, which should be modeled as 2D CD sources.

Involving more parameters, estimators for 2D CD sources have higher computational complexity. Extended form DSPE for 1D CD sources, Zhang et al. [12] have proposed a spectral search approach for 2D CD sources with L-shape arrays. Utilizing double parallel linear arrays (DPLA), treble parallel linear arrays (TPLA), and conformal arrays, several low-complexity algorithms have been opined in [13–18], where estimations of DOAs are performed under ESPRIT or propagator framework based on approximate rotational invariance relationships of steering vectors. Lee et al. [19] have proposed a sequential one-dimensional searching algorithm based on double uniform circular arrays (DUCA). In [20], DOAs can be estimated from proposed symmetric properties of a centrosymmetric crossed array. Considering CD sources are correlated with each other, Wu et al. [21] have made a proposition of a 2D estimator utilizing DPLA. Based on L-shaped arrays, Wu et al,[22] have explored the estimation of a 2D nonsymmetric CD source, where nonsymmetric ASDF is established by a Gaussian mixture model.

Aforementioned methods mostly are proposed based on uniform arrays where the separations between sensors are limited to the value no more than half proportion of the wavelength of impinging signal. In the context of point source estimation, in order to achieve the greatest levels of accuracy as well as to have more sources resolved, larger apertures should be used; consequently, a larger number of sensors are required. Although point sources and distributed sources are different targets, the traditional estimators for distributed source also requires the separations between sensors not greater than half wavelength, and the estimation accuracy is closely related to the aperture size. The nested arrays which have been proposed in [23] tend to have greater degree of freedoms (DOFs) as well as huge apertures. Aiming at point sources, DOA estimators with diverse types of nested arrays have been explored in [24–29]. In [29], Zheng et al. have presented an estimator resolving near-field (NF) and far-field (FF) point sources simultaneously using a symmetric double nested array (SDNA). Zheng and Mu [30] have proposed a 2D DOA estimator using two parallel nested arrays where an augmented covariance matrix is constructed to reduce computational complexity. The coprime arrays composed of ULAs with sensor spacing related by a cprime integer have been proposed in [31]. Shi et al. [32] have presented 2D DOA estimation with coprime planar arrays (CPPAs) which achieve a great increase of aperture and reduce computational complexity by virtue of iterative scheme for transforming 2D grids searching into 1D searching during sparse representation. In [33], Zheng et al. have proposed a new sparse array called configuration maximum interelement spacing constraint (MISC) array where the array structure is designed in terms of the interelement spacing set, which is given in a closed-form expression as a function of the number of sensors.

Compared with estimators for a point source model, the researches of estimators for distributed sources under sparse arrays are relatively few and most of these studies deal with 1D distributed source. Estimators for 1D exponential distributed sources based on the linear nested array have been presented in [34] with a prior knowledge of angular spreads and without the prior knowledge in [35]. Considering 2D ID sources, Wu et al. [36] have developed a sparse representation method under nested array, where computational complexity is extremely high.

In this paper, based on a proposed nested array containing double parallel linear subarrays, a DOA estimator for 2D CD sources is presented. By means of vectorization operation on the cross-correlation matrices, double hole-free virtual uniform linear arrays are realized and the closed expressions of virtual sensor coordinates are deduced based on the difference coarray concept. Next, rotational invariance relationships of virtual arrays are deduced. Based on rotational invariance relationships, matrices satisfying rotation invariance are constructed by extracting and regrouping the receive vectors of the virtual arrays. Then, an ESPRIT-like framework based on matrix reconstruction is proposed. The proposed method can detect 2D CD sources more than sensors without angles matching and without prior knowledge of ASDF. Lastly, the effectiveness of the

proposed method is investigated through simulations. To show the contributions of this paper clearly, the main differences between the state-of-the-art methods and our work are listed as follows:

(i) Though DOA estimations for 2D CD sources are presented in [12–22], the arrays are all uniform. In [27, 28, 30, 32], DOA estimators for 2D sources using sparse arrays are considered, which aim at point sources. In [34, 35], estimators for 1D exponential distributed sources based on nested arrays are established, while 2D distributed sources are more general and accordant with practical circumstances. In this paper, estimation for 2D CD sources with the nested array is considered.

(ii) A nested array used for 2D sources is proposed. Configuration of virtual arrays containing close form of virtual sensor positions, maximum DOF, and the optimal parameters get deduced. Compared with uniform linear arrays for 2D sources, the nested array proposed has larger aperture as well as more DOFs.

(iii) A matrix reconstruction algorithm is detailed based on an ESPRIT-like framework on matrices which is constructed by extracting receive vectors of the virtual arrays. Without angles matching and without prior knowledge of ASDF, the algorithm proposed has less computation complexity than existing methods using uniform arrays.

Notations. Scalar variables are denoted by italic letters, and vectors and matrices are denoted by bold letters. $(\bullet)^{-1}$, $(\bullet)^{*}$, $(\bullet)^{T}$, and $(\bullet)^{H}$ mean inverse, complex conjugate, transpose, and Hermitian transpose of a matrix. $E[\bullet]$, $(./)$, $\text{vec}(\bullet)$, $\odot$ and $(\bullet)+$ denote expectation, element-wise division, vectorization, Khatri–Rao product and pseudoinverse operation. $[\bullet]_k$ is the kth element of a vector. $\text{diag}[\bullet]$ means diagonal matrix. $\arg(\bullet)$ is the phase of a complex number.

2. The Nested Array and Source Model

As illustrated in Figure 1, double parallel uniform subarrays $A1$ and $A2$ on the xoz plane constitute a nested array. Parallel to x-axis, $A1$ is made up of a middle sensor on z-axis and M_1 sensors are separated by d meters on both sides. Subarray $A2$ is on x-axis containing M_2 sensors located on both semiaxes with sensor spacing $D = (2M_1 + 1)d$. The interval of the two subarrays equals $d/2$. q 2D CD sources with wavelength λ and nominal angles (θ_i, φ_i) $(i = 1, 2, \ldots, q)$ in the far field are set to be estimated, $\theta_i \in [0, \pi]$, $\varphi_i \in [0, \pi]$. θ_i is a denotation of the spatial nominal azimuth that exists between x positive semiaxes and the propagation path of the ith source. φ_i is the nominal elevation of the source. The consideration of noise is the Gaussian white zero mean which is an additive as well as uncorrelated with sensors.

The sensor coordinate set of subarrays $A1$ and $A2$ can be expressed, respectively, as

$$\mathscr{C}_1 = \left\{ (l_m d, 0, 0.5d) \,\middle|\, l_m = -M_1, -(M_1 - 1), \ldots, (M_1 - 1), M_1 \right\}, \tag{1}$$

$$\mathscr{C}_2 = \left\{ (l_n + 0.5)D, 0, 0) \,\middle|\, l_n = -M_2, -(M_2 - 1), \ldots, (M_2 - 1) \right\}. \tag{2}$$

Receive vectors of subarrays $A1$ and $A2$ have the following expressions:

$$\mathbf{x}_1(t) = \sum_{i=1}^{q} \iint \boldsymbol{\eta}_1(\theta, \varphi) s_i(\theta, \varphi, t) \mathrm{d}\theta \mathrm{d}\varphi + \mathbf{n}_{x1}(t), \tag{3}$$

$$\mathbf{x}_2(t) = \sum_{i=1}^{q} \iint \boldsymbol{\eta}_2(\theta, \varphi) s_i(\theta, \varphi, t) \mathrm{d}\theta \mathrm{d}\varphi + \mathbf{n}_{x2}(t), \tag{4}$$

where $\mathbf{n}_{x1}(t)$ and $\mathbf{n}_{x2}(t)$ are noise vectors. $\boldsymbol{\eta}_1(\theta, \varphi)$ and $\boldsymbol{\eta}_2(\theta, \varphi)$ denote the steering vectors of subarrays $A1$ and $A2$, which have the following expressions:

$$\boldsymbol{\eta}_1(\theta, \phi) = e^{j\pi d \cos\phi/\lambda} \left[e^{-j2\pi M_1 d \cos\theta/\lambda}, e^{-j2\pi (M_1 - 1) d \cos\theta/\lambda}, \ldots, 1, \ldots, e^{j2\pi (M_1 - 1) d \cos\theta/\lambda}, e^{j2\pi M_1 d \cos\theta/\lambda} \right]^T. \tag{5}$$

$$\boldsymbol{\eta}_2(\theta, \phi) = \left[e^{-j2\pi (M_2 - 0.5) D \cos\theta/\lambda}, e^{-j2\pi (M_2 - 1.5) D \cos\theta/\lambda}, \ldots, e^{j2\pi (M_2 - 1.5) D \cos\theta/\lambda}, e^{j2\pi (M_2 - 0.5) D \cos\theta/\lambda} \right]^T. \tag{6}$$

$s_i(\theta, \varphi, t)$ in equations (3) and (4) represents angular signal density function of the ith 2D CD source. Based on the assumption of the CD source, $s_i(\theta, \varphi, t)$ can be written as

$$s_i(\theta, \varphi, t) = s_i(t) g(\theta, \varphi; \mathbf{u}_i), \tag{7}$$

where $s_i(t)$ reflects time behavior of the ith source. $g_i(\theta, \varphi; \mathbf{u}_i)$ represents deterministic ASDF of the ith source reflecting spatial distribution of scatterers with respect to the ith source. A 2D deterministic ASDF is generally characterized by the parameter vector $\mathbf{u}_i = [\theta_i, \varphi_i, \sigma_{\theta i}, \sigma_{\varphi i}]^T$ with four elements which are nominal azimuth θ_i, nominal elevation φ_i, azimuth angular spread $\sigma_{\theta i}$, and elevation angular spread $\sigma_{\varphi i}$.

Deterministic ASDF of a Gaussian CD source has the following expression:

$$g(\theta, \varphi; \mathbf{u}_i) = \frac{1}{2\pi\sigma_{\theta i}\sigma_{\phi i}} \exp\left\{ -0.5 \left[\left(\frac{\theta - \theta_i}{\sigma_{\theta i}} \right)^2 + \left(\frac{\phi - \phi_i}{\sigma_{\phi i}} \right)^2 \right] \right\}. \tag{8}$$

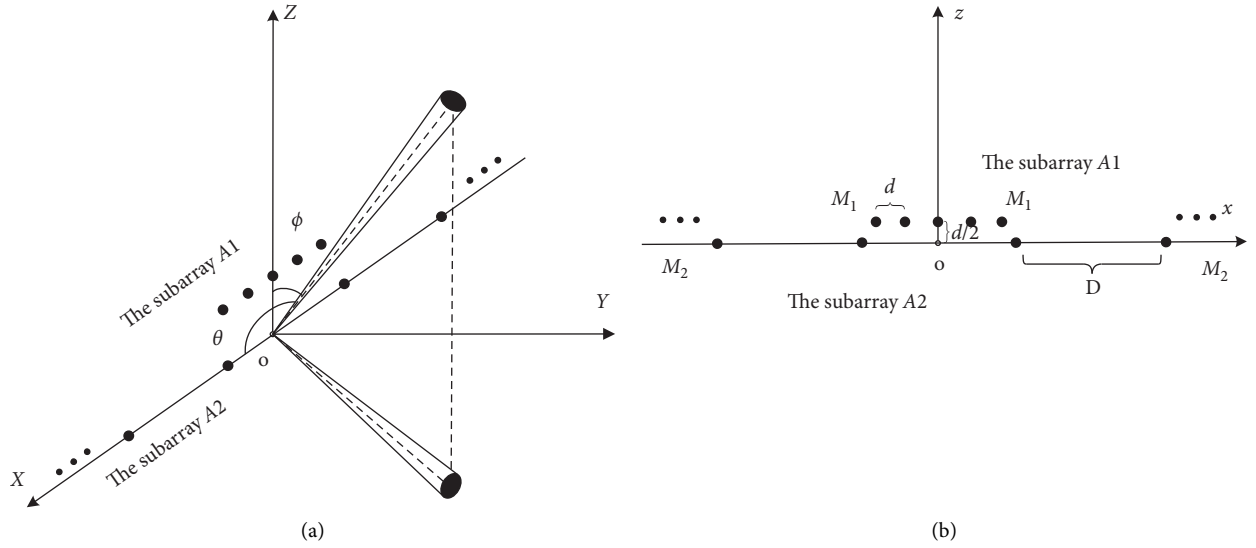Deterministic ASDF of a uniform CD source have the following expression:

Figure 1: (a) Configuration of the nested array proposed; (b) illustration of the array proposed on the *xoz* plane.

$$g\left(\theta, \varphi; \mathbf{u}_i\right) = \begin{cases} \dfrac{1}{4\sigma_{\theta i}\sigma_{\phi i}}, & \left|\theta - \theta_i\right| \le \sigma_{\theta i} \text{ and } \left|\phi - \phi_i\right| \le \sigma_{\phi i}, \\ \\ 0, & \left|\theta - \theta_i\right| \ge \sigma_{\theta i} \text{ or } \left|\phi - \phi_i\right| \ge \sigma_{\phi i}. \end{cases} \tag{9}$$

3. Proposed Method

This part is composed of four portions. Firstly, double parallel virtual uniform linear arrays are realized through difference operation. Then, the rotational invariance relationship of virtual arrays gets deduced. Afterwards, matrices satisfying rotation invariance are constructed using the receive vectors of the virtual arrays and a matrix

reconstruction algorithm based on an ESPRIT-like framework is proposed. The procedure of computation gets summarized as well as the analysis of the complexity is performed by comparing other methods with traditional uniform arrays.

3.1. Description of Virtual Arrays. The nested array increases DOFs by forming virtual arrays through difference operation between sensor coordinates of subarrays. $(2M_1 + 1) \times 2M_2$ dimensional matrix $\mathbf{R}_1$ is denoted as the cross-correlation matrix of subarrays $A1$ and $A2$ and the $2M_2 \times (2M_1 + 1)$ dimensional matrix $\mathbf{R}_2$ as the cross-correlation matrix of subarrays $A2$ and $A1$. As different CD sources are uncorrelated, $\mathbf{R}_1$ and $\mathbf{R}_2$ can be expressed as follows:

$$\mathbf{R}_1 = E\left[\mathbf{x}_1(t)\mathbf{x}_2^H(t)\right] = \sum_{i=1}^{q} \sigma_i^2 \int\int \boldsymbol{\eta}_1(\theta, \varphi) g(\theta, \varphi; \mathbf{u}_i) g(\theta, \varphi; \mathbf{u}_i) \boldsymbol{\eta}_2^H(\theta, \varphi) \mathrm{d}\theta \mathrm{d}\varphi, \tag{10}$$

$$\mathbf{R}_2 = E\left[\mathbf{x}_2(t)\mathbf{x}_1^H(t)\right] = \sum_{i=1}^{q} \sigma_i^2 \int\int \boldsymbol{\eta}_2(\theta, \varphi) g(\theta, \varphi; \mathbf{u}_i) g(\theta, \varphi; \mathbf{u}_i) \boldsymbol{\eta}_1^H(\theta, \varphi) \mathrm{d}\theta \mathrm{d}\varphi, \tag{11}$$

where $\sigma_i^2 = E[|s_i(t)|^2]$ is the power of the ith source. Vectorizing $\mathbf{R}_1$ and $\mathbf{R}_2$ by the Khatri–Rao product, we have

$$\bar{\mathbf{r}}_1 = \mathrm{vec}\left(\mathbf{R}_1\right) = \sum_{i=1}^{q} \sigma_i^2 \int\int \boldsymbol{\eta}_2^*(\theta, \varphi) \odot \boldsymbol{\eta}_1(\theta, \varphi) g(\theta, \varphi; \mathbf{u}_i) g(\theta, \varphi; \mathbf{u}_i) \mathrm{d}\theta \mathrm{d}\varphi, \tag{12}$$

$$\bar{\mathbf{r}}_2 = \mathrm{vec}\left(\mathbf{R}_2\right) = \sum_{i=1}^{q} \sigma_i^2 \int\int \boldsymbol{\eta}_1^*(\theta, \varphi) \odot \boldsymbol{\eta}_2(\theta, \varphi) g(\theta, \varphi; \mathbf{u}_i) g(\theta, \varphi; \mathbf{u}_i) \mathrm{d}\theta \mathrm{d}\varphi. \tag{13}$$

Double parallel virtual uniform linear arrays can be obtained by vectorization of cross-correlation matrices $\mathbf{R}_1$ and $\mathbf{R}_2$ which is illustrated in Figure 2. Through difference operation between sensor coordinates of subarrays $A1$ and $A2$, virtual arrays VA and VB can be realized with sensor coordinate sets $\mathbb{C}_A$ and $\mathbb{C}_B$ expressed as

$$\mathbb{C}_A = \left\{ \mathbf{p}_i - \mathbf{p}_j \,\middle|\, \mathbf{p}_i \in \mathbb{C}_1, \mathbf{p}_j \in \mathbb{C}_2 \right\}, \qquad (14)$$

$$\mathbb{C}_B = \left\{ \mathbf{p}_j - \mathbf{p}_i \,\middle|\, \mathbf{p}_i \in \mathbb{C}_1, \mathbf{p}_j \in \mathbb{C}_2 \right\}. \qquad (15)$$

From equations (1) and (2), we have sensor coordinate sets of the virtual arrays $\mathbb{C}_A$ and $\mathbb{C}_B$ as

$$\mathbb{C}_A = \left\{ [(n - 0.5)d, 0, 0.5\,d] \,\middle|\, n = 1 - (2M_1M_2 + M_2), 2 - (2M_1M_2 + M_2), \ldots, 2M_1M_2 + M_2) \right\}, \qquad (16)$$

$$\mathbb{C}_B = \left\{ [(n - 0.5)d, 0, -0.5\,d] \,\middle|\, n = 1 - (2M_1M_2 + M_2), 2 - (2M_1M_2 + M_2), \ldots, 2M_1M_2 + M_2) \right\}. \qquad (17)$$

Equations (16) and (17) show that each virtual array contains $L = 2(2M_1M_2 + M_2)$ virtual sensors without repetitive positions, which indicates both virtual arrays formed by nested array are hole-free. It is worth noting that the element sequence in $\bar{\mathbf{r}}_1$ does not correspond to sensor orders of virtual array VA; meanwhile, the element sequence in $\bar{\mathbf{r}}_2$ does not correspond to sensor orders of VB. $\mathbf{r}_A$ is denoted as receive signal vector with elements reflecting signal received from the virtual sensor located on $[(0.5 - 2M_1M_2 - M_2)d, 0, 0.5d]$ to the sensor located on $[(2M_1M_2 + M_2 - 0.5)d, 0, 0.5d]$ and $\mathbf{r}_B$ as receive signal vector with elements reflecting signal received from the virtual sensor located on $[(0.5 - 2M_1M_2 - M_2)d, 0, -0.5d]$ to the sensor

located on $[(2M_1M_2 + M_2 - 0.5)d, 0, -0.5d]$. After reordering $\bar{\mathbf{r}}_1$ and $\bar{\mathbf{r}}_2$, $\mathbf{r}_A$ and $\mathbf{r}_B$ can be expressed as

$$\mathbf{r}_A = \sum_{i=1}^{q} \sigma_i^2 \int\int \mathbf{a}(\theta, \varphi) g(\theta, \varphi; \mathbf{u}_i) g(\theta, \varphi; \mathbf{u}_i) d\theta d\varphi, \qquad (18)$$

$$\mathbf{r}_B = \sum_{i=1}^{q} \sigma_i^2 \int\int \mathbf{b}(\theta, \varphi) g(\theta, \varphi; \mathbf{u}_i) g(\theta, \varphi; \mathbf{u}_i) d\theta d\varphi, \qquad (19)$$

where $\mathbf{a}(\theta, \varphi)$ and $\mathbf{b}(\theta, \varphi)$ denote the $L \times 1$ dimensional steering vector of virtual arrays VA and VB, which have the following expressions:

$$\mathbf{a}(\theta, \varphi) = e^{j\pi d\cos\varphi/\lambda} \left[e^{-j2\pi(2M_1M_2 + M_2 - 0.5)d\cos\theta/\lambda}, e^{-j2\pi(2M_1M_2 + M_2 - 1.5)d\cos\theta/\lambda}, \ldots, e^{j2\pi(2M_1M_2 + M_2 - 0.5)d\cos\theta/\lambda} \right]^T, \qquad (20)$$

$$\mathbf{b}(\theta, \varphi) = e^{-j\pi d\cos\varphi/\lambda} \left[e^{-j2\pi(2M_1M_2 + M_2 - 0.5)d\cos\theta/\lambda}, e^{-j2\pi(2M_1M_2 + M_2 - 1.5)d\cos\theta/\lambda}, \ldots, e^{j2\pi(2M_1M_2 + M_2 - 0.5)d\cos\theta/\lambda} \right]^T. \qquad (21)$$

In the process of estimation, the sample of covariance matrix with N snapshots can be substituted for $\mathbf{R}_1$ and $\mathbf{R}_2$ as follows:

$$\widehat{R}_1 = \frac{1}{N} \sum_{t=1}^{N} \left[\mathbf{x}_1(t) \mathbf{x}_2^H(t) \right],$$

$$\widehat{R}_2 = \frac{1}{N} \sum_{t=1}^{N} \left[\mathbf{x}_2(t) \mathbf{x}_1^H(t) \right]. \qquad (22)$$

3.2. Rotational Invariance Relationships of Virtual Arrays.
Representing response of arrays to the ith distributed source, generalized steering vectors are defined in [10]. The generalized steering vector $\boldsymbol{\alpha}_i$ reflects response of array VA to the ith CD source while the generalized steering vector $\boldsymbol{\beta}_i$ reflects response of array VB to the source. $\boldsymbol{\alpha}_i$ and $\boldsymbol{\beta}_i$ can be written as

$$\boldsymbol{\alpha}_i = \int\int \mathbf{a}(\theta, \varphi) g(\theta, \varphi; \mathbf{u}_i) g(\theta, \varphi; \mathbf{u}_i) d\theta d\varphi, \qquad (23)$$

$$\boldsymbol{\beta}_i = \int\int \mathbf{b}(\theta, \varphi) g(\theta, \varphi; \mathbf{u}_i) g(\theta, \varphi; \mathbf{u}_i) d\theta d\varphi. \qquad (24)$$

Each element of $\boldsymbol{\alpha}_i$ or $\boldsymbol{\beta}_i$ represents the response of corresponding virtual sensor of VA and VB to the ith CD source. Representing response of arrays to all distributed sources, $\mathbf{A}$ and $\mathbf{B}$ are defined as $L \times q$ dimensional generalized steering matrices of the virtual arrays VA and VB, which can be written as

$$\mathbf{A} = \left[\boldsymbol{\alpha}_1, \boldsymbol{\alpha}_2, \ldots, \boldsymbol{\alpha}_q \right], \qquad (25)$$

$$\mathbf{B} = \left[\boldsymbol{\beta}_1, \boldsymbol{\beta}_2, \ldots, \boldsymbol{\beta}_q \right]. \qquad (26)$$

$\boldsymbol{\sigma}$ is denoted as a power vector of CD sources, which can be expressed as

$$\boldsymbol{\sigma} = \left[\sigma_1^2, \sigma_2^2, \ldots, \sigma_q^2 \right]^T. \qquad (27)$$

Thus, $\mathbf{r}_A$ and $\mathbf{r}_B$ can be expressed as

$$\mathbf{r}_A = \mathbf{A}\boldsymbol{\sigma}, \qquad (28)$$

$$\mathbf{r}_B = \mathbf{B}\boldsymbol{\sigma}. \qquad (29)$$

If d/λ is set at 1/2, the following relationships can be obtained under the condition that angular spreads of CD sources are small (the proof can be seen in Appendix):
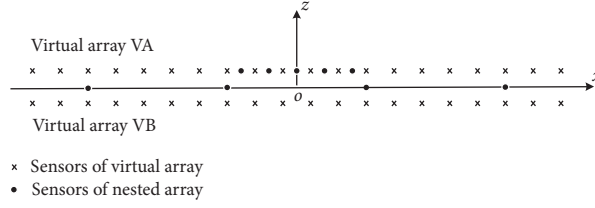
FIGURE 2: Virtual arrays formed by nested array.

$$[\boldsymbol{\alpha}_i]_{k+1} \approx e^{j\pi\cos\theta_i} [\boldsymbol{\alpha}_i]_k, \tag{30}$$

$$[\boldsymbol{\beta}_i]_{k+1} \approx e^{j\pi\cos\theta_i} [\boldsymbol{\beta}_i]_k, \tag{31}$$

$$[\boldsymbol{\alpha}_i]_k \approx e^{j\pi\cos\varphi_i} [\boldsymbol{\beta}_i]_k. \tag{32}$$

Therefore, rotational invariance relationships can be drawn as follows:

$$[\mathbf{A}]_{k+1} \approx [\mathbf{A}]_k \boldsymbol{\Phi}, \tag{33}$$

$$[\mathbf{B}]_{k+1} \approx [\mathbf{B}]_k \boldsymbol{\Phi}, \tag{34}$$

$$[\mathbf{A}]_k \approx [\mathbf{B}]_k \boldsymbol{\Psi}, \tag{35}$$

where the rotational invariance operators $\boldsymbol{\Phi}$ and $\boldsymbol{\Psi}$ can be written as

$$\boldsymbol{\Phi} = \operatorname{diag}\left[e^{j\pi\cos\theta_1}, e^{j\pi\cos\theta_2}, \ldots, e^{j\pi\cos\theta_q}\right], \tag{36}$$

$$\boldsymbol{\Psi} = \operatorname{diag}\left[e^{j\pi\cos\varphi_1}, e^{j\pi\cos\varphi_2}, \ldots, e^{j\pi\cos\varphi_q}\right]. \tag{37}$$

3.3. DOA Estimation via Matrix Reconstruction.
Receive vectors described by equations (28) and (29) can be considered q coherent power signals impinging into virtual arrays VA and VB. In this paper, according to the concept of ESPRIT, matrices satisfying rotation invariance are constructed by extracting and regrouping the receive vectors of the virtual arrays.

Defining $\mathbf{r}_A^1$ as the receive vector of the first q elements of $\mathbf{r}_A$ and $\mathbf{r}_B^1$ as the receive vector of the first q elements of $\mathbf{r}_B$, we have

$$\mathbf{r}_A^1 = \mathbf{A}_1 \boldsymbol{\sigma}, \tag{38}$$

$$\mathbf{r}_B^1 = \mathbf{B}_1 \boldsymbol{\sigma}, \tag{39}$$

where $\mathbf{A}_1$ and $\mathbf{B}_1$ are generalized steering matrices of $\mathbf{r}_A^1$ and $\mathbf{r}_B^1$. $\mathbf{A}_1$ and $\mathbf{B}_1$ can be expressed as

$$\mathbf{A}_1 = \begin{bmatrix} \mathbf{I}_{q\times q} & \mathbf{0}_{q\times(L-q)} \end{bmatrix} \mathbf{A}, \tag{40}$$

$$\mathbf{B}_1 = \begin{bmatrix} \mathbf{I}_{q\times q} & \mathbf{0}_{q\times(L-q)} \end{bmatrix} \mathbf{B}, \tag{41}$$

where $\mathbf{I}_{q\times q}$ is the $q \times q$ dimensional identity matrix and $\mathbf{0}_{q\times(L-q)}$ is the $q \times (L-q)$ dimensional null matrix. The operation $\begin{bmatrix} \mathbf{I}_{q\times q} & \mathbf{0}_{q\times(L-q)} \end{bmatrix}$ left multiply A or B can be considered as extracting the first q rows of a matrix.

According to equations (33)–(35), a generalized steering matrix of the receive vector of ith q elements of $\mathbf{r}_A$ and $\mathbf{r}_B$ can be expressed as

$$\mathbf{A}_i \approx \mathbf{A}_1 \boldsymbol{\Phi}^{i-1}, \quad i = 1, 2, \ldots, q+1, \tag{42}$$

$$\mathbf{B}_i \approx \mathbf{B}_1 \boldsymbol{\Phi}^{i-1}, \quad i = 1, 2, \ldots, q+1, \tag{43}$$

$$\mathbf{B}_1 \approx \mathbf{A}_1 \boldsymbol{\Psi}. \tag{44}$$

Then, the receive vector of ith q elements of $\mathbf{r}_A$ and $\mathbf{r}_B$ can be expressed as

$$\mathbf{r}_A^i = \mathbf{A}_i \boldsymbol{\sigma} \approx \mathbf{A}_1 \boldsymbol{\Phi}^{i-1} \boldsymbol{\sigma}, \tag{45}$$

$$\mathbf{r}_B^i = \mathbf{B}_i \boldsymbol{\sigma} \approx \mathbf{B}_1 \boldsymbol{\Phi}^{i-1} \boldsymbol{\sigma}. \tag{46}$$

A $q \times q$ dimensional matrix $\mathbf{R}_A'$ is constructed in the way that $\mathbf{r}_A^i$ is converted into the ith column of $\mathbf{R}_A'$. Another $q \times q$ dimensional matrix $\mathbf{R}_A''$ is reconstructed in the way that $\mathbf{r}_A^{i+1}$ is converted into the ith columns of $\mathbf{R}_A''$. Thus, $\mathbf{R}_A'$ and $\mathbf{R}_A''$ can be written as follows:

$$\mathbf{R}_A' = \sum_{i=1}^{q} \mathbf{r}_A^i \mathbf{e}_i^T = \mathbf{A}_1 \boldsymbol{\Lambda} \sum_{i=1}^{q} \mathbf{Q}^{i-1} \mathbf{e}_i^T = \mathbf{A}_1 \boldsymbol{\Lambda} \mathbf{A}_1^H, \tag{47}$$

$$\mathbf{R}_A'' = \sum_{i=2}^{q+1} \mathbf{r}_A^i \mathbf{e}_i^T = \mathbf{A}_1 \boldsymbol{\Lambda} \sum_{i=2}^{q+1} \mathbf{Q}^{i-1} \mathbf{e}_i^T = \mathbf{A}_1 \boldsymbol{\Phi} \boldsymbol{\Lambda} \mathbf{A}_1^H, \tag{48}$$

where $\boldsymbol{\Lambda} = \operatorname{diag}[\sigma_1^2, \sigma_2^2, \ldots, \sigma_q^2]$ and $\mathbf{Q} = [e^{j\pi\cos\theta_1}, e^{j\pi\cos\theta_2}, \ldots, e^{j\pi\cos\theta_q}]^T$. $\mathbf{e}_i = [0, \ldots, 1, 0, \ldots]$ is the q dimensional vector with 1 as the ith element and 0 as others, which can be seen as an operator transforming a vector into a column in a matrix.

Similarly, $\mathbf{R}_B'$ is constructed in the way that $\mathbf{r}_B^i$ is converted into the ith column of the matrix.

$$\mathbf{R}_B' = \sum_{i=1}^{q} \mathbf{r}_B^i \mathbf{e}_i^T = \mathbf{B}_1 \boldsymbol{\Lambda} \sum_{i=1}^{q} \mathbf{Q}^{i-1} \mathbf{e}_i^T = \mathbf{B}_1 \boldsymbol{\Lambda} \mathbf{A}_1^H = \mathbf{A}_1 \boldsymbol{\Psi} \boldsymbol{\Lambda} \mathbf{A}_1^H, \tag{49}$$

where $\mathbf{A}_1^H$ is a Vandermonde full rank matrix and $\boldsymbol{\Lambda}$ is a diagonal matrix. From equations (48) and (49), we have

$$(\mathbf{R}_A')^+ \mathbf{R}_A'' = \mathbf{A}_1 \boldsymbol{\Phi} \mathbf{A}_1^{-1}, \tag{50}$$

$$(\mathbf{R}_A')^+ \mathbf{R}_B' = \mathbf{A}_1 \boldsymbol{\Psi} \mathbf{A}_1^{-1}. \tag{51}$$

$(\mathbf{R}_A')^+ \mathbf{R}_A''$ and $(\mathbf{R}_A')^+ \mathbf{R}_B'$ are denoted as $\boldsymbol{\Omega}_1$ and $\boldsymbol{\Omega}_2$, respectively. The rotational invariance operators $\boldsymbol{\Phi}$ and $\boldsymbol{\Psi}$ are

diagonal matrices. According to equations (50) and (51), the eigenvectors corresponding to the elements in the same position in the two diagonal matrices $\mathbf{\Phi}$ and $\mathbf{\Psi}$ are the same, which means eigenvalue $e^{j\pi\cos\theta_i}$ of $\mathbf{\Omega}_1$ and eigenvalue $e^{j\pi\cos\varphi_i}$ of $\mathbf{\Omega}_2$ have a same eigenvector. Therefore, once we obtain $e^{j\pi\cos\theta_i}$ through eigendecomposition of $\mathbf{\Omega}_1$, eigenvectors corresponding to $e^{j\pi\cos\theta_i}$ can be substituted in (51) to calculate the $e^{j\pi\cos\varphi_i}$ paired with $e^{j\pi\cos\theta_i}$.

We can obtain eigenvalue μ_i $(i = 1, 2, \ldots, q)$ of $\mathbf{\Omega}_1$ and its corresponding eigenvectors ξ_i by means of eigendecomposition. Then, we can obtain the nominal azimuth as follows:

$$\theta_i = \arccos\frac{\arg(\mu_i)}{\pi}, \quad i = 1, 2, \ldots, q. \tag{52}$$

As corresponding eigenvalues of $\mathbf{\Omega}_1$ and $\mathbf{\Omega}_2$ have the same eigenvector, without angles matching, eigenvalue of $\mathbf{\Omega}_2$ can be obtained as follows:

$$\nu_i = \frac{1}{q}\mathbf{1}_{1\times q} \cdot [(\mathbf{\Omega}_2\xi_i) \cdot /\xi_i], \tag{53}$$

where $\mathbf{1}_{1\times q}$ is the $1 \times q$ dimensional vector with all elements as 1 and $(./)$ denotes element-wise division. $(\mathbf{\Omega}_2\xi_i)$ equals $\nu_i\xi_i$ as the ith eigenvalue μ_i of $\mathbf{\Omega}_1$, and the ith eigenvalue ν_i of $\mathbf{\Omega}_2$ has the same eigenvector. The operation of element-wise division between $(\mathbf{\Omega}_2\xi_i)$ and ξ_i obtains a $q \times 1$ dimensional vector with all elements equal to ν_i theoretically.

Then, we can obtain the nominal elevation as follows:

$$\phi_i = \arccos\frac{\arg(\nu_i)}{\pi}, \quad i = 1, 2, \ldots, q. \tag{54}$$

3.4. Analysis of the Nested Array. Based on the analysis of Section 3.3, maximum number of unknown CD sources q can achieve half of the virtual sensors of each virtual arrays; thus, DOF of the arrays proposed is $(2M_1M_2 + M_2)$; total sensor number of the array is $M = 2(M_1 + M_2) + 1$. We can draw the conclusion that DOF of the nested array proposed can reach $O(M^2)$ and the DOF is far more than the total sensor number. We examine the maximum DOF that can be achieved, and the maximum goal under the given total sensor number can be written as

$$\begin{aligned}\max &\quad 2M_1M_2 + M_2 \\ \text{subject to} &\quad M = 2(M_1 + M_2) + 1.\end{aligned} \tag{55}$$

We obtain

$$\begin{aligned}M_1^{\text{opt}} &= \frac{M}{4} - \frac{1}{2}, \\ M_2^{\text{opt}} &= \frac{M}{4}.\end{aligned} \tag{56}$$

As M_1^{opt} and M_2^{opt} could be fractions, M_1, M_2, and $(M-1)/2$ are all integers, and optimal solutions should be modified. Refer to the definition in [29], coarray aperture of the proposed nested array is defined as physical length in x dimension multiply physical length in z dimension of virtual arrays. Table 1 shows maximum DOF and the coarray aperture of the optimal configuration.

We analyze DOFs of the method proposed in comparison with representative existing methods for 2D CD sources with the same sensor number M which are DSPE using a L-shape array [12], modified propagator (MP) using TPLA, [15] and SOS using DUCA [19]. According to the optimal configuration described in Table 1, DOFs of the method proposed are shown in Figure 3. It can be seen that the nested arrays proposed have a larger number of DOFs than uniform arrays with the same sensor number.

The algorithm proposed can be performed according to Table 2.

We analyze the computational complexity of the method proposed in comparison with representative existing methods for 2D CD sources based on uniform arrays with the same sensor number M which are DSPE using a L-shape array [12], Modified Propagator (MP) using TPLA [15], and SOS using DUCA [19]. Computational cost of DSPE using a L-shape array [12] mainly lies in computing the sample covariance matrix $O(NM^2)$, pseudoinverse operation of the covariance matrix $O(M^3)$, and four-dimensional searching $O(M^3K^4)$, where K denotes search points of unknown parameters. Computational cost of MP using TPLA [15] mainly lies in computing the modified propagator $O(NM^2)$ and inversion as well as eigendecomposition of the sample covariance matrix $O(M^3)$, obtaining rotational invariance matrices $O(q^3)$. SOS using DUCA [19] is an algorithm based on 1D searching; computational cost mainly lies in computing the sample covariance matrix $O(NM^2)$ and inversion as well as eigendecomposition of the sample covariance matrix $O(M^3)$, one-dimensional searching $O(M^3K)$. The computational cost of the method proposed mostly lie in computing the sample covariance matrix $O(NM^2)$, calculation of pseudoinversion of $\mathbf{R}_A'$ which is $O(q^3)$, and eigendecomposition of $\mathbf{\Omega}_1$ and $\mathbf{\Omega}_2$ which is $O(q^3)$. As $M > q$, the computation complexity of the proposed method is far less than existing methods for 2D CD sources using uniform arrays.

Remark 1. The advantages of the proposed method lies in that the proposed arrays have larger aperture as well as more DOFs compared with traditional estimators for CD sources based on uniform arrays with similar number of sensors. Compared with existing estimators for CD sources based on nested arrays, the proposed method can estimate 2D CD sources and the estimation can be performed without prior knowledge of ASDF of sources as well as spectral searching.

Remark 2. The method proposed is not suitable for 2D CD sources which are coherent with each other. A CD source is defined as the scatterers of a source which are coherent; meanwhile, the sources are incoherent. In other words signals emitted from scatterers within a source are coherent while signals from scatterers from different sources are incoherent. Under the condition that CD sources are incoherent, we can obtain R_1 and R_2 in the forms of (10) and (11) which are the basis of vectorization to obtain the virtual receive vector of virtual arrays.

Remark 3. Although the array structure proposed achieves aperture expansion in both the elevation and azimuth

TABLE 1: Maximum DOF and the coarray aperture of the optimal configuration.

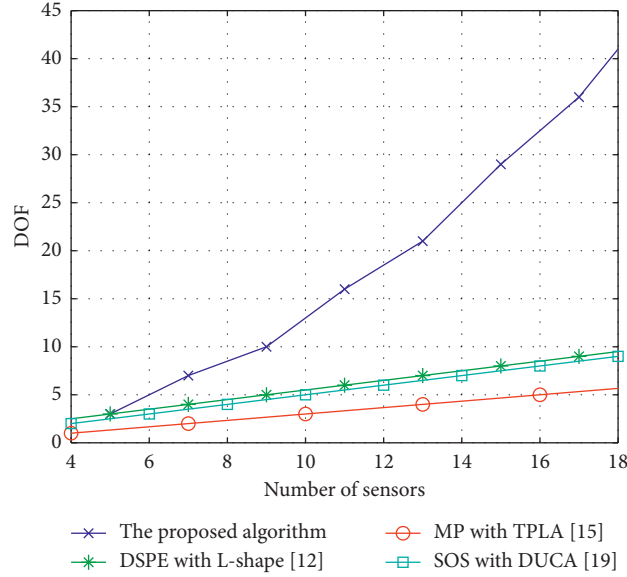| N (n is an integer)	M_1	M_2	DOF	Coarray aperture
$4n + 1$	N	n	$2n^2 + n$	$(4n^2 + 2n - 1)d \times d$
$4n + 3$	N	$n + 1$	$2n^2 + 3n + 2$	$(4n^2 + 6n + 1)d \times d$

FIGURE 3: DOFs of different methods.

TABLE 2: Summary of the proposed method.

Input: N snapshots of receive vectors of the subarrays A_1 and A_2 array $\{\mathbf{x}_1(t)\}_{t=1}^{N}$ and $\{\mathbf{x}_2(t)\}_{t=1}^{N}$
Output: nominal angles of q 2D CD sources (θ_i, φ_i) ($i = 1, 2, \ldots, q$).

(1) Computing the sample cross-correlation matrix of subarrays $\mathbf{R}_1$ and $\mathbf{R}_2$ from equations (22).
(2) Vectorizing $\mathbf{R}_1$ and $\mathbf{R}_2$ from equations (12) and (13) and reordering sequences of elements in vectors $\bar{r}_1$ and $\bar{r}_2$ to obtain $\mathbf{r}_A$ and $\mathbf{r}_B$.
(3) Extracting the elements of vectors $\mathbf{r}_A$ and $\mathbf{r}_B$ to get $\mathbf{r}_A^i$ and $\mathbf{r}_B^i$ and constructing $\mathbf{R}_A'$, $\mathbf{R}_A''$, and $\mathbf{R}_B'$ form equations (47)–(49).
(4) Calculation and eigendecomposition of $\mathbf{\Omega}_1$ and $\mathbf{\Omega}_2$.
(5) Computing nominal elevation θ_i from equation (52) and nominal elevation φ_i from equation (54).

dimensions, the aperture expansion in the elevation direction is limited. In addition, rotational invariance relationship is an approximate resolution under small angular spread assumption; when the sensor number is bigger, later sensors in the virtual array are a result of more transitive relationships. The abovementioned two factors indicate that the proposed method can improve the estimation accuracy of DOA of 2D CD sources to a certain extent.

4. Results and Discussion

Three numerical simulation experiments are carried out to investigate the effectiveness of the proposed algorithm in this section. The root mean squared error (RMSE) of the ith source with regard to DOA can be written as

$$\text{RMSE}_{\theta_i} = \sqrt{\frac{1}{\text{Mc}} \sum_{\zeta}^{\text{Mc}} \left(\widehat{\theta}_i^{\zeta} - \theta_i \right)^2}, \qquad (57)$$

$$\text{RMSE}_{\varphi_i} = \sqrt{\frac{1}{\text{Mc}} \sum_{\zeta}^{\text{Mc}} \left(\widehat{\varphi}_i^{\zeta} - \varphi_i \right)^2}, \qquad (58)$$

where $\widehat{\theta}_i^{\varsigma}$ and $\widehat{\varphi}_i^{\varsigma}$ are the estimated nominal azimuth and elevation of the ith source where ς means the estimated value in the ςth Monte Carlo run. Mc is the total number of Monte Carlo simulations. The signal-to-noise ratio (SNR) is defined as $10\log(1/\sigma^2)$ where the noise is assumed to be the Gaussian white zero mean with variance σ^2.

In the first example, we investigate the performance of the method proposed, considering the underdetermined scenario. Figure 4(a) demonstrates that 16 2D CD sources distributed uniformly from diamond area from (30°, 81°), (72°, 40°) to (114°, 81°), (72°, 122°) are set to be estimated. The nested array is set with $M_1 = 2$, $M_2 = 3$, $M = 11$, and $d = \lambda/2$. Angular spreads are 2°, SNR = 5 dB, the number of snapshots equal to 300, and Mc = 100. An indicator reflecting the number of sources detected is needed to measure the
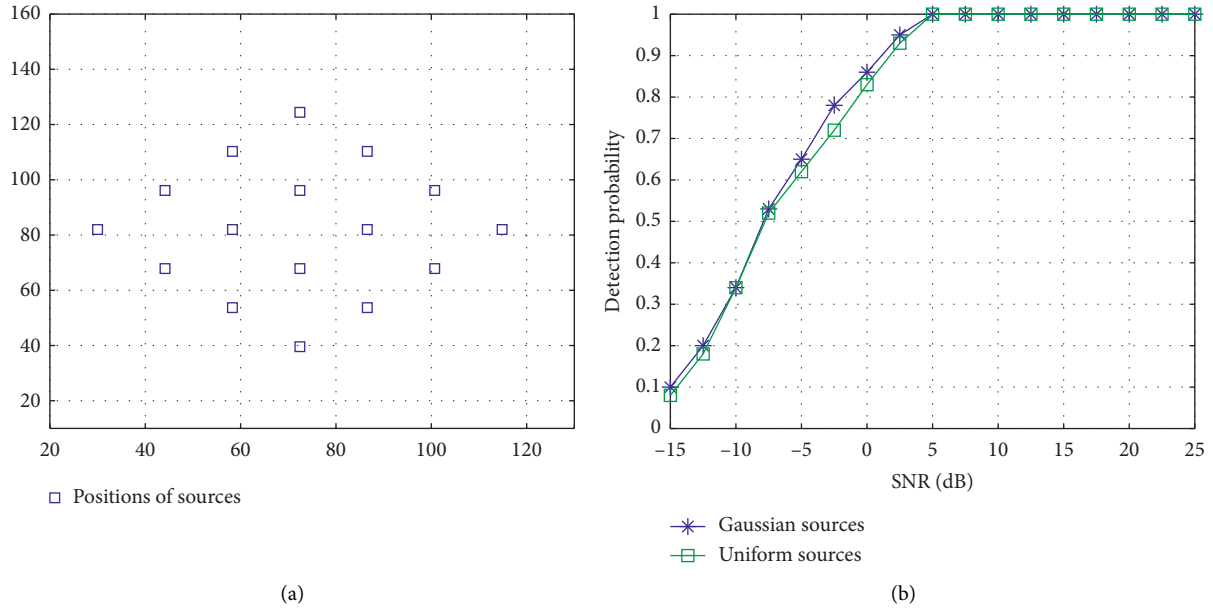
(a)

(b)

FIGURE 4: (a) Location of 2D CD sources to be estimated; (b) detection probability versus SNR.

performance of different estimators. In the first trial, all 16 sources are Gaussian while in the second trial are uniform. Detection probability is defined as $N_d/16$ where N_d is the number of sources estimated effectively. Estimation is regarded as effective when the estimated angles satisfy $[(\widehat{\theta}_i - \theta_i)^2 + (\widehat{\phi}_i - \phi_i)^2]^{0.5} \leq 5°$. Figure 4(b) exhibits the detection probability with change of SNR. As can be seen from Figure 4(b), all the 2D CD sources can be detected when SNR exceeds 5 dB whether sources are Gaussian or uniform. Detection probability decreases as SNR decreases. The difference of detection probability between the two types of CD sources is not significant. This example demonstrated that the nested array and algorithm proposed can resolve 2D CD sources in undermining circumstances.

In the second example, we investigate the performance of the method proposed with regard to angular spreads of sources. Based on the assumption that angular spreads of sources are small rotational invariance relationships that get deduced, the influence of angular spreads on the estimation should be investigated. Both Gaussian and uniform sources are considered, respectively. Experiments are set with $M_1 = 1$, $M_2 = 1$, $M = 5$, $d = \lambda/2$, Mc = 100, SNR = 5 dB, and the number of snapshots equal to 300. Nominal angles of sources are (35°, 35°) and (145°, 145°). Angular spreads of sources are set from 0° to 10°. RMSE is replaced by the mean values of RMSE_{θ_i} and RMSE_{φ_i} of two sources. As shown in Figure 5, RMSE reaches 0.58° when angular spreads are 10° for Gaussian sources, while RMSE reaches 0.73° when angular spreads reach 10° for uniform sources. It is obvious that estimated results deteriorate for both kinds of sources as the angular spreads increase. The estimation performance is still satisfactory within 10°. The method proposed exhibits robustness under the condition of small angular spreads. Estimation of the method proposed can be conducted without prior knowledge of ASDF and can also be demonstrated.

In the third example, we investigate the performance of the method proposed versus SNR and the number of snapshots. Gaussian CD sources with centers (35°, 35°) and (145°, 145°) are set to be estimated. Angular spreads are 2°. Nested array configuration is the same as example 2, Mc = 100. RMSE takes mean values of sources. Experiments are conducted in comparison with existing methods for 2D CD sources based on the L-shape array [12] with 5 sensors, MP using TPLA [15] with 7 sensors, and SOS using DUCA [19] with 6 sensors, respectively. Figure 6(a) shows simulation results as well as the Cramer–Rao bound (CRB) [37] while SNR is ranging from −5 dB to −30 dB with the number of snapshots set at 300. Figure 6(b) shows simulation results as well as CRB with the number of snapshots ranging from 200 to 1000 while SNR is fixed at 5 dB. Figure 6 shows that RMSE of all methods decrease with either SNR increase or number of snapshots increase, and the method proposed has lower RMSE than others. The method proposed illustrates greater performance than the traditional methods with similar sensor number under the same experimental conditions. The reason probably lies in that the nested array possesses larger aperture than uniform arrays with similar number of sensors.

In the fourth example, we investigate the performance of the proposed method versus sensor number M. The sensor number of subarrays $A1$ and $A2$ is set according to the optimal configuration described in Table 1. Both Gaussian and uniform sources are considered, respectively. The sources to be estimated in the first trial are Gaussian with nominal angles (35°, 35°) and (145°, 145°) while in the second trial are uniform with the same nominal angles as the first trail. RMSE takes the mean values of sources. Figure 7 shows simulation results with the number of total sensors ranging from 5 to 19 while SNR is fixed at 5 dB and the number of snapshots fixed at 300. Angular spreads are 2°, $d = \lambda/2$. It can be concluded that the proposed method provides better
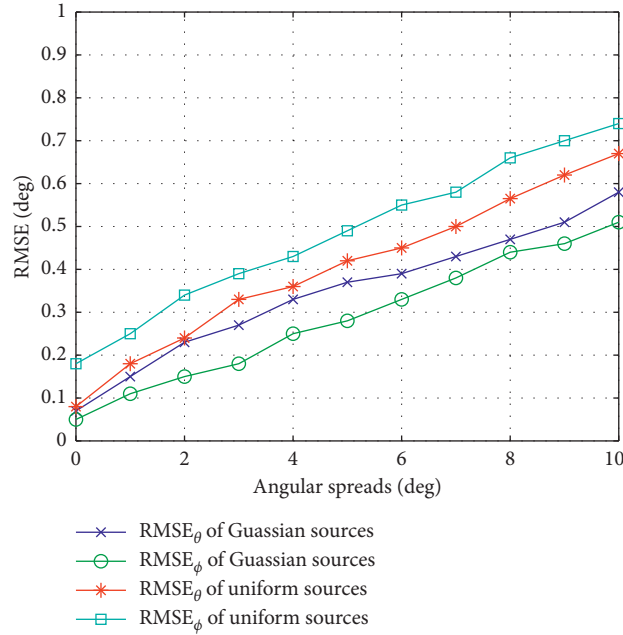
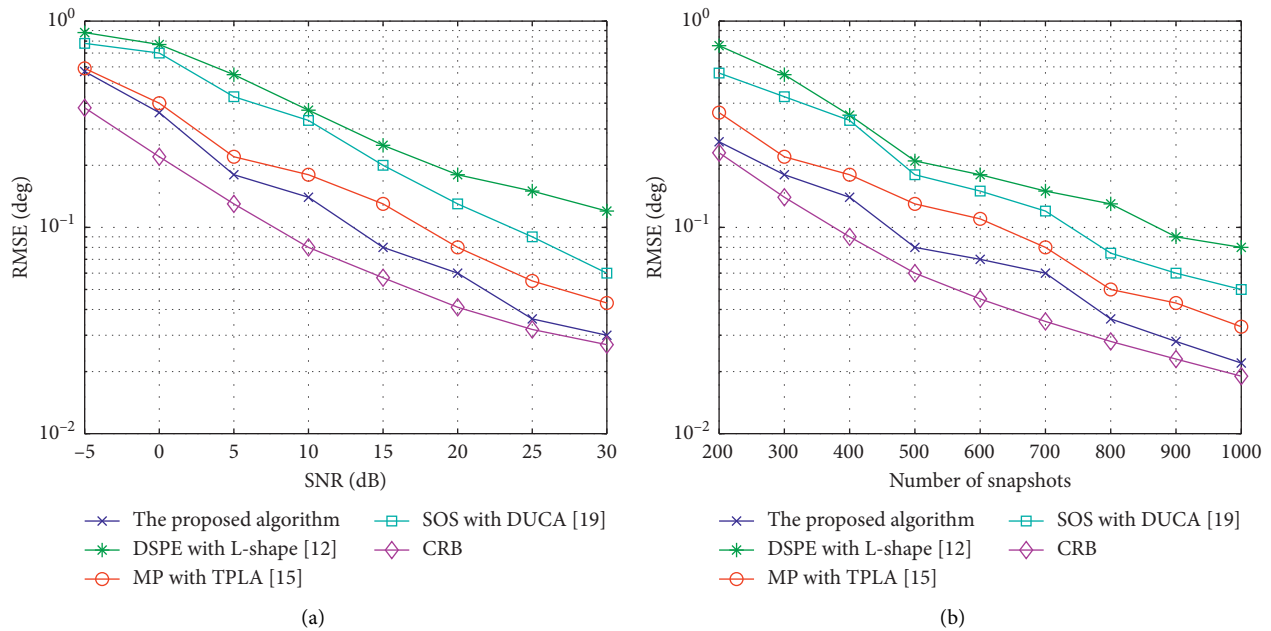Figure 5: RMSE estimated for 2D CD sources versus angular spreads.

Figure 6: (a) Estimation of the method proposed versus SNR; (b) estimation of the method proposed versus number of snapshots.

performance for both kinds of 2D CD sources as the sensor number increases, but RMSE changes slightly when the total sensor number increases to a certain extent. The reason mainly lies in that the rotational invariance relationship is an approximate resolution under small angular spreads assumption. When the sensor number is bigger,

on one hand, the coarray aperture increases which is advantageous to the estimation performance; on the other hand, later sensors in the virtual array is a result of more transitive relationships, which means the proposed method can improve the estimation accuracy to a certain extent.
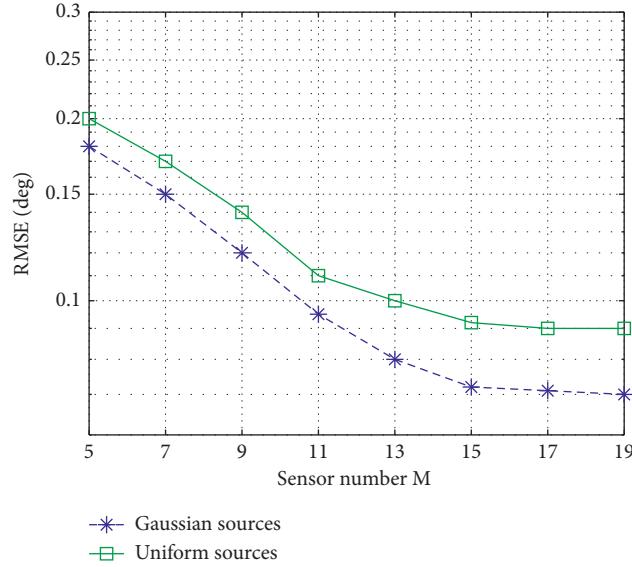
FIGURE 7: Estimation of the method proposed versus the total sensor number M.

5. Conclusion

Aiming at DOA of 2D CD sources, a 2D nested array as well as an estimation algorithm is proposed in this paper. According to the difference coarray concept, double parallel hole-free virtual uniform linear arrays are obtained by vectorization operation on cross-correlation matrices of subarrays. Configuration of virtual arrays containing close form of sensor coordinates, maximum DOF, and the optimal parameters get deduced. Rotational invariance relationships of virtual arrays are derived under the condition that angular spreads of sources are small. A matrix reconstruction algorithm is detailed based on an ESPRIT-like framework on matrices constructed by extracting and regrouping the receive vectors of the virtual arrays. Numerical simulations considering underdetermined scenario, angular spread, the influence of experiment, and total sensor number are conducted. Outcomes illustrated that the method proposed can deal with more sources than sensors without prior knowledge of ASDF as well as exhibit higher accuracy than uniform arrays under the same experimental conditions.

Appendix

Checking $[\boldsymbol{\alpha}_i]_k$ and $[\boldsymbol{\alpha}_i]_{k+1}$ of equation (30), d/λ is set at $1/2$. Replacing variables $(\theta_i + \widetilde{\theta})$ with θ and $(\phi_i + \widetilde{\phi})$ with φ, where $\widetilde{\theta}$ and $\widetilde{\varphi}$ are the small deviations of θ_i and ϕ_i, $\cos\theta$ and $\cos\varphi$ can be approximated by the first term in the Taylor series expansions. $[\boldsymbol{\alpha}_i]_k$ and $[\boldsymbol{\alpha}_i]_{k+1}$ can be respectively expressed as follows:

$$
\begin{aligned}
[\boldsymbol{\alpha}_i]_k &= \iint e^{j0.5\pi\cos\varphi} e^{-j\pi\left(2M_1M_2+M_2-k+0.5\right)\cos\theta} g\left(\theta,\varphi;\mathbf{u}_i\right) g\left(\theta,\varphi;\mathbf{u}_i\right) \mathrm{d}\theta \mathrm{d}\varphi \\
&= \iint e^{j0.5\pi\left(\cos\varphi_i-\sin\varphi_i\widetilde{\varphi}\right)} e^{-j\pi\left(2M_1M_2+M_2-k+0.5\right)\left(\cos\theta_i-\sin\theta_i\widetilde{\theta}\right)} \left[g\left(\theta_i+\widetilde{\theta},\varphi_i+\widetilde{\varphi};\mathbf{u}_i\right)\right]^2 \mathrm{d}\widetilde{\theta}\mathrm{d}\widetilde{\varphi} \\
&= e^{j0.5\pi\cos\varphi_i} e^{-j\pi\left(2M_1M_2+M_2-k+0.5\right)\cos\theta_i} \iint e^{-j0.5\pi\sin\varphi_i\widetilde{\varphi}} e^{j\pi\left(2M_1M_2+M_2-k+0.5\right)\sin\theta_i\widetilde{\theta}} \left[g\left(\theta_i+\widetilde{\theta},\varphi_i+\widetilde{\varphi};\mathbf{u}_i\right)\right]^2 \mathrm{d}\widetilde{\theta}\mathrm{d}\widetilde{\varphi},
\end{aligned}
\tag{A.1}
$$

$$
\begin{aligned}
[\boldsymbol{\alpha}_i]_{k+1} &= \iint e^{j0.5\pi\cos\varphi} e^{-j\pi\left(2M_1M_2+M_2-k-0.5\right)\cos\theta} g\left(\theta,\varphi;\mathbf{u}_i\right) g\left(\theta,\varphi;\mathbf{u}_i\right) \mathrm{d}\theta \mathrm{d}\varphi \\
&= \iint e^{j0.5\pi\left(\cos\varphi_i-\sin\varphi_i\widetilde{\varphi}\right)} e^{-j\pi\left(2M_1M_2+M_2-k-0.5\right)\left(\cos\theta_i-\sin\theta_i\widetilde{\theta}\right)} \left[g\left(\theta_i+\widetilde{\theta},\varphi_i+\widetilde{\varphi};\mathbf{u}_i\right)\right]^2 \mathrm{d}\widetilde{\theta}\mathrm{d}\widetilde{\varphi} \\
&= e^{j0.5\pi d\cos\varphi_i} e^{-j\pi\left(2M_1M_2+M_2-k-0.5\right)\cos\theta_i} \iint e^{-j0.5\pi\sin\varphi_i\widetilde{\varphi}} e^{j\pi\left(2M_1M_2+M_2-k+0.5\right)\sin\theta_i\widetilde{\theta}} e^{-j\pi\sin\theta_i\widetilde{\theta}} \left[g\left(\theta_i+\widetilde{\theta},\varphi_i+\widetilde{\varphi};\mathbf{u}_i\right)\right]^2 \widetilde{\theta}\mathrm{d}\widetilde{\varphi}.
\end{aligned}
\tag{A.2}
$$

Under the assumption of small angular spreads, it follows that $e^{-j\pi \sin \theta_i \theta} \approx 1$, so $[\boldsymbol{\alpha}_i]_{k+1}$ can be written as

$$[\boldsymbol{\alpha}_i]_{k+1} \approx e^{j\pi \cos \theta_i} [\boldsymbol{\alpha}_i]_k. \qquad (A.3)$$

The proof of equation (31) is similar to equation (30). Considering equation (32),

$$
\begin{aligned}
[\boldsymbol{\beta}_i]_k &= \iint e^{-j0.5\pi \cos \varphi} e^{-j\pi \left(2M_1 M_2 + M_2 - k + 0.5\right) \cos \theta} g\left(\theta, \varphi; \mathbf{u}_i\right) g\left(\theta, \varphi; \mathbf{u}_i\right) \mathrm{d}\theta \mathrm{d}\varphi \\
&= \iint e^{-j0.5\pi \left(\cos \varphi_i - \sin \varphi_i \widetilde{\varphi}\right)} e^{-j\pi \left(2M_1 M_2 + M_2 - k + 0.5\right) \left(\cos \theta_i - \sin \theta_i \widetilde{\theta}\right)} \left[g\left(\theta_i + \widetilde{\theta}, \varphi_i + \widetilde{\varphi}; \mathbf{u}_i\right)\right]^2 \mathrm{d}\widetilde{\theta} \mathrm{d}\widetilde{\varphi} \\
&= e^{-j0.5\pi \cos \varphi_i} e^{-j\pi \left(2M_1 M_2 + M_2 - k + 0.5\right) \cos \theta_i} \iint e^{j0.5\pi \sin \varphi_i \widetilde{\varphi}} e^{j\pi \left(2M_1 M_2 + M_2 - k + 0.5\right) \sin \theta_i \widetilde{\theta}} \left[g\left(\theta_i + \widetilde{\theta}, \varphi_i + \widetilde{\varphi}; \mathbf{u}_i\right)\right]^2 \mathrm{d}\widetilde{\theta} \mathrm{d}\widetilde{\varphi}. \qquad (A.4)
\end{aligned}
$$

Under the assumption of small angular spreads, it follows that $e^{-j\pi \sin \varphi_i \widetilde{\varphi}} \approx 1$, so $[\boldsymbol{\alpha}_i]_k$ can be written as

$$[\boldsymbol{\alpha}_i]_k \approx e^{j\pi \cos \varphi_i} [\boldsymbol{\beta}_i]_k. \qquad (A.5)$$

Data Availability

The data used to support the findings of this study are available from the corresponding author upon reasonable request via e-mail address taowu_nwpu@126.com.

Conflicts of Interest

The authors declare no conflicts of interest.

Acknowledgments

References

[1] S. Valaee, B. Champagne, and P. Kabal, "Parametric localization of distributed sources," *IEEE Transactions on Signal Processing*, vol. 43, no. 9, pp. 2144–2153, 1995.

[2] H. Chen, C. Hou, W. Liu, W.-P. Zhu, and M. N. S. Swamy, "Efficient two-dimensional direction-of-arrival estimation for a mixture of circular and noncircular sources," *IEEE Sensors Journal*, vol. 16, no. 8, pp. 2527–2536, 2016.

[3] H. Chen, C. Hou, W.-P. Zhu et al., "ESPRIT-like two-dimensional direction finding for mixed circular and strictly noncircular sources based on joint diagonalization," *Signal Processing*, vol. 141, pp. 48–56, 2017.

[4] F. Wen, J. Shi, and Z. Zhang, "Joint 2D-DOD, 2D-DOA, and polarization angles estimation for bistatic EMVS-MIMO radar via PARAFAC analysis," *IEEE Transactions on Vehicular Technology*, vol. 69, no. 2, pp. 1626–1638, 2020.

[5] X. P. Wang, L. T. Wan, M. X. Huang, C. Shen, Z. G. Han, and T. Zhu, "Low-complexity channel estimation for circular and noncircular signals in virtual MIMO vehicle communication systems," *IEEE Transactions on Vehicular Technology*, vol. 69, no. 4, pp. 3916–3928, 2020.

[6] Z. Zheng, W.-Q. Wang, H. Meng, H. C. So, and H. Zhang, "Efficient beamspace-based algorithm for two-dimensional DOA estimation of incoherently distributed sources in massive MIMO systems," *IEEE Transactions on Vehicular Technology*, vol. 67, no. 12, pp. 11776–11789, 2018.

[7] Y. Meng, P. Stoica, and K. M. Wong, "Estimation of direction of arrival of spatially dispersed signals in array processing," *IEE Proceedings—Radar, Sonar and Navigation*, vol. 143, no. 1, pp. 1–9, 1996.

[8] Q. Wu, K. M. Wong, and Y. Meng, "DOA estimation of point and scattered sources—vet-Music," in *Proceedings of the IEEE Seventh SP Workshop on Statistical Signal and Array Processing*, Quebec, QC, Canada, June 1994.

[9] S. Shahbazpanahi, S. Valaee, and M. H. Bastani, "Distributed source localization using ESPRIT algorithm," *IEEE Transactions on Signal Processing*, vol. 49, no. 10, pp. 2169–2178, 2001.

[10] A. Zoubir, Y. Wang, and P. Charge, "New adaptive beamformers for estimation of spatially distributed sources," in *Proceedings of the IEEE Antennas and Propagation Society International Symposium*, Monterey, CA, USA, June 2004.

[11] W. Xiong, P. José, and S. Marcos, "Performance analysis of distributed source parameter estimator (DSPE) in the presence of modeling errors due to the spatial distributions of sources," *Signal Processing*, vol. 143, pp. 146–151, 2018.

[12] G. M. Zhang, H. G. Wang, and C. L. Zhang, "A parameter estimation method of 2D distributed source based on L-shape uniform array," *Technical Acoustics*, vol. 33, pp. 204–208, 2014.

[13] X. Guo, Q. Wan, W. Yang, and X. Lei, "Low-complexity 2D coherently distributed sources decoupled DOAs estimation method," *Science in China Series F: Information Sciences*, vol. 52, no. 5, pp. 835–842, 2009.

[14] Z. Zheng, G. Li, and Y. Teng, "Simplified estimation of 2D DOA for coherently distributed sources," *Wireless Personal Communications*, vol. 62, no. 4, pp. 907–922, 2012.

[15] Z. Zheng, G. Li, and Y. Teng, "2D DOA Estimator for multiple coherently distributed sources using modified propagator," *Circuits, Systems, and Signal Processing*, vol. 31, no. 1, pp. 255–270, 2012.

[16] Z. Zheng, G. J. Li, and Y. Teng, "Low-complexity method for the 2D DOA decoupled estimation of coherently distributed sources," *Chinese Journal of Radio Science*, vol. 25, pp. 527–533, 2010.

[17] Z. Zheng, G. Li, and Y. Teng, "Low-complexity 2D DOA estimator for multiple coherently distributed sources," *COMPEL—The International Journal for Computation and Mathematics in Electrical and Electronic Engineering*, vol. 31, no. 2, pp. 443–459, 2012.

[18] L. Wan, G. Han, J. Jiang, C. Zhu, and L. Shu, "A DOA estimation approach for transmission performance guarantee in D2D communication," *Mobile Networks and Applications*, vol. 22, no. 6, pp. 998–1009, 2017.

[19] J. Lee, I. Song, H. Kwon, and S. Ro Lee, "Low-complexity estimation of 2D DOA for coherently distributed sources," *Signal Processing*, vol. 83, no. 8, pp. 1789–1802, 2003.

[20] Z. Dai, W. Cui, B. Ba, D. Wang, and Y. Sun, "Two-dimensional DOA estimation for coherently distributed sources with symmetric properties in crossed arrays," *Sensors*, vol. 17, no. 6, p. 1300, 2017.

[21] T. Wu, X. Zhang, Y. Li, Z. Deng, and Y. Huang, "On spatial smoothing for DOA Estimation of 2D coherently distributed sources with double parallel linear arrays," *Electronics*, vol. 8, no. 3, p. 354, 2019.

[22] T. Wu, Z. H. Deng, and Q. Y. Gu, "Estimation for two-dimensional nonsymmetric coherently distributed source in L-shaped arrays," *International Journal of Antennas and Propagation*, vol. 2018, Article ID 5247919, 16 pages, 2018.

[23] P. Pal and P. P. Vaidyanathan, "Nested arrays: a novel approach to array processing with enhanced degrees of freedom," *IEEE Transactions on Signal Processing*, vol. 58, no. 8, pp. 4167–4181, 2010.

[24] P. Alinezhad, S. R. Seydnejad, and D. Abbasi-Moghadam, "DOA estimation in conformal arrays based on the nested array principles," *Digital Signal Processing*, vol. 50, pp. 191–202, 2016.

[25] Y. Tian, Q. Lian, and H. Xu, "Mixed near-field and far-field source localization utilizing symmetric nested array," *Digital Signal Processing*, vol. 73, pp. 3–14, 2017.

[26] E. Boudaher, F. Ahmad, M. G. Amin, and A. Hoorfar, "Mutual coupling effect and compensation in non-uniform arrays for direction-of-arrival estimation," *Digital Signal Processing*, vol. 61, pp. 3–14, 2017.

[27] Y. Y. Dong, C. X. Dong, Y.-T. Zhu, G.-Q. Zhao, and S. Y. Liu, "Two-dimensional DOA estimation for L-shaped array with nested subarrays without pair matching," *IET Signal Processing*, vol. 10, no. 9, pp. 1112–1117, 2016.

[28] W. Si, Z. Peng, C. Hou, and F. Zheng, "Two-dimensional DOA estimation for three-parallel nested subarrays via sparse representation," *Sensors*, vol. 18, no. 6, p. 1861, 2018.

[29] Z. Zheng, M. Fu, W.-Q. Wang, S. Zhang, and Y. Liao, "Localization of mixed near-field and far-field sources using symmetric double-nested arrays," *IEEE Transactions on Antennas and Propagation*, vol. 67, no. 11, pp. 7059–7070, 2019.

[30] Z. Zheng and S. Mu, "Two-dimensional DOA estimation using two parallel nested arrays," *IEEE Communications Letters*, vol. 24, no. 3, pp. 568–571, 2020.

[31] P. P. Vaidyanathan and P. Pal, "Sparse sensing with co-prime samplers and arrays," *IEEE Transactions on Signal Processing*, vol. 59, no. 2, pp. 573–586, 2011.

[32] J. Shi, G. Hu, X. Zhang, F. Sun, and H. Zhou, "Sparsity-based two-dimensional DOA estimation for coprime array: from sum-difference coarray viewpoint," *IEEE Transactions on Signal Processing*, vol. 65, no. 21, pp. 5591–5604, 2017.

[33] Z. Zheng, W.-Q. Wang, Y. Kong, and Y. D. Zhang, "MISC array: a new sparse array design achieving increased degrees of freedom and reduced mutual coupling effect," *IEEE Transactions on Signal Processing*, vol. 67, no. 7, pp. 1728–1741, 2019.

[34] K. Han and A. Nehorai, "Nested array processing for distributed sources," *IEEE Signal Processing Letters*, vol. 21, no. 9, pp. 1111–1114, 2014.

[35] C. Wen, G. Shi, and X. Xie, "Estimation of directions of arrival of multiple distributed sources for nested array," *Signal Processing*, vol. 130, pp. 315–322, 2017.

[36] T. Wu, Y. W. Li, Z. X. Li, Y. J. Huang, and J. W. Xu, "A 2D nested array based DOA estimator for incoherently distributed sources via sparse representation utilizing l_1-norm," *International Journal of Antennas and Propagation*, vol. 2019, Article ID 6941963, 11 pages, 2019.

[37] G. Y. Zhang and B. Tang, "Decoupled estimation of 2D DOA for coherently distributed sources using 3D matrix pencil method," *EURASIP Journal on Advances in Signal Processing*, vol. 2008, Article ID 417157, 7 pages, 2008.